On-board data processing for the Near Infrared Spectrograph and Photometer instrument (NISP) of the EUCLID mission

Carlotta Bonoli*[a], Andrea Balestra[a], Favio Bortoletto[a], Maurizio D'Alessandro[a], Ruben Farinelli[a], Eduardo Medinaceli[a], John Stephen[e],
Enrico Borsato[b,c], Stefano Dusini[b], Fulvio Laudisio[b,d], Chiara Sirignano[b,c], Sandro Ventura[b]
Natalia Auricchio[e], Leonardo Corcione[f], Enrico Franceschi[e], Sebastiano Ligori[f],
Gianluca Morgante[e], Laura Patrizii[g], Gabriele Sirri[g], Massimo Trifoglio[e], Luca Valenziano[e]

[a]INAF, Osservatorio Astronomico di Padova, vicolo Osservatorio 5, 35122 Padova, Italy;
[b]Istituto Nazionale di Fisica Nucleare sezione di Padova, via Marzolo 8, 35131 Padova, Italy;
[c]Dipartimento di Fisica e Astronomia, Università degli Studi di Padova, via Marzolo 8, 35131 Padova, Italy;
[d]CISAS, Università degli Studi di Padova, Via Venezia 15, 35131 Padova, Italy;
[e]INAF, IASF Bologna, via Piero Gobetti, 101, 40129 Bologna, Italy;
[f]INAF, Osservatorio Astronomico di Torino, Strada Osservatorio 20, 10025 Torino, Italy;
[g]Istituto Nazionale di Fisica Nucleare sezione di Bologna, Viale B. Pichat 6/2, 40127 Bologna, Italy

ABSTRACT

The Near Infrared Spectrograph and Photometer (NISP) is one of the two instruments on board the EUCLID mission now under implementation phase; VIS, the Visible Imager is the second instrument working on the same shared optical beam. The NISP focal plane is based on a detector mosaic deploying 16x, 2048x2048 pixels^2 HAWAII-II HgCdTe detectors, now in advanced delivery phase from Teledyne Imaging Scientific (TIS), and will provide NIR imaging in three bands (Y, J, H) plus slit-less spectroscopy in the range 0.9÷2.0 micron.
All the NISP observational modes will be supported by different parametrization of the classic multi-accumulation IR detector readout mode covering the specific needs for spectroscopic, photometric and calibration exposures.
Due to the large number of deployed detectors and to the limited satellite telemetry available to ground, a consistent part of the data processing, conventionally performed off-line, will be accomplished on board, in parallel with the flow of data acquisitions.
This has led to the development of a specific on-board, HW/SW, data processing pipeline, and to the design of computationally performing control electronics, suited to cope with the time constraints of the NISP acquisition sequences during the sky survey.
In this paper we present the architecture of the NISP on-board processing system, directly interfaced to the SIDECAR ASICs system managing the detector focal plane, and the implementation of the on-board pipe-line allowing all the basic operations of input frame averaging, final frame interpolation and data-volume compression before ground down-link.

Keywords: space, simulations, on-board data processing.

1. INTRODUCTION

Euclid is a wide-field space mission concept dedicated to the high-precision probing of dark energy and dark matter. It will carry out an imaging and spectroscopic wide survey of the entire extra-galactic sky (20000 deg^2) along with a deep

*carlotta.bonoli@oapd.inaf.it; phone +39 049 8293481; fax +39 049 8759

survey covering 10-100 deg^2. To achieve these science objectives the current Euclid reference design consists of a wide field telescope to be placed in L2 orbit by a Soyuz launch in 2020 with a 6 year mission lifetime. The payload consists of a 1.2m diameter 3-mirror telescope light feeding two instruments: a visible domain imager instrument (VIS) and a near infrared domain spectrometer/photometer instrument (NISP). Both instruments will observe, simultaneously, the same Field of View on the sky. The overall payload system design is optimized for a sky survey in a step-and-stare tiling mode.
Differently from the visual channel the NISP instrument, based on a 4x4 IR detectors focal plane implements on board pre-processing on exposures sampled by non-destructive readouts to obtain the final science frame.
In order to study the performance of the spectrograph and to drive the requirements on the various instrument parameters, we developed an end-to-end scheme for the on-board processing operations that allows detailed comparison of different readout strategies based on realistic characteristics of the detectors and having in mind the achievement of the expected mission scientific goals. The present NISP instrument pre-processing concept and test results obtained during the ongoing phase C are here presented.

2. MISSION SURVEY DATA PRODUCTS

The NISP survey[5] foresees a continuous scanning of the sky outside the galactic plane in step and stare pointed fields, each composed by four exposures sequences separated by small pointing dithering to allow correction of effects like inter-detector blind gaps and cosmic-ray discrimination[1].

Each dithered sequence, as reported in Figure 1, is covered by one spectrograph exposure followed by three photometric exposures in different spectral bands. In such a way the total number of exposures obtained per field is subdivided in the following mode :

1. NIS Spectrograph : 4x exposures each with a different Red Grism orientation
2. NIP Photometer : 12x exposures (3x bands on the four dithered sequences)

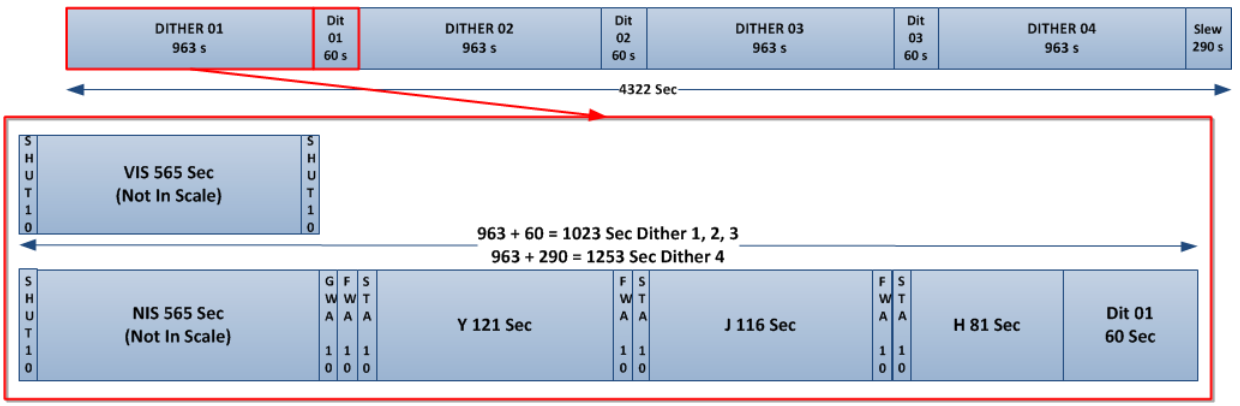

Figure 1. Structure of a single NISP observation field on top and expansion of the first dithered sequence. A maximum of 19 fields can be allocated per day. To be noticed, during the NIS exposure the parallel activity of the VIS Visible camera on the same pointed field.

Each fourth dithered sequence is also terminated with a dark exposure allowing systematic monitoring of detectors pedestal and persistence and providing information valuable for further on-ground processing. This is specifically the case of post mitigation of previously accumulated persistence on incoming data.

*carlotta.bonoli@oapd.inaf.it; phone +39 049 8293481; fax +39 049 8759

Exposures are made in the standard '*multi-accumulation*' mode (MACC[2]). Multi-accumulation exposure programming takes advantage from the high flexibility provided by the Teledyne H2RG[3] SCA (Sensor Chip Assembly) and SCE (Sensor Chip Electronics, namely the Teledyne Sidecar[3]) combination allowing, by simple setting of a few parameters in the exposure command, to span from Fowler to full Up the Ramp (UTR) mode of readout with, obviously, different total exposure time in combination with the number of required intermediate non-destructive frames.
The needed exposure parameter, as from the specific NISP implementation for the SCE flight microcode, are:

1. The number of initial reset frames
2. The delay from last reset to first collected frame (in steps of D_{L1} detector lines, here assumed = 2048)
3. The number of groups of frames interleaved during the exposure N_G
4. The number of consecutive frames acquired in each group N_F
5. The delay between programmed groups of frames (in steps of D_{L2} detector lines)

Under the above assumptions the total resulting exposure time is:

$$Texp = \left(D_{L1} + D_{L2} \times (N_G - 1)\right) \times L_T + N_G \times N_F \times F_T$$

where : $L_T = 689 \times 10^{-6}\ s$ is the readout line time and, $F_T = 1.41s$, is the readout frame time.

The presently assumed Multi-accumulation parameters and amount of produced data in terms of frames and bytes per single detector and exposure are as in Table 1, while the resulting exposure times are reported in Figure 1. As from the table a not negligible part of produced data is made by a sub-set of detector lines (5 per detector) located at specified coordinates and aimed to monitor the detector behavior during exposures. They are sent to ground un-processed and un-compressed.

Table 1. Amount of data per single detector and single exposure during the nominal NISP survey activity. Raw detector lines are in number of 5, extracted from all incoming readouts and stacked for all detectors produced frames without associated processing nor compression. They are meant to monitor, on ground, the behavior of original, untouched, pixels from the focal plane.

Exp Mode :	Groups N_G:	Frames/ Group NF:	Inter-Group Line Drops:	Resulting Frames:	Total GBytes:	Raw Lines Mbytes:	Resulting Exp. (S):
Spectro	15	16	23864	240	2	4.92	565
Photo Y	4	16	14200	64	0.54	1.31	121
Photo J	4	16	12000	64	0.54	1.31	116
Photo H	3	16	8990	48	0.40	1.00	81
Dark	4	16	14200	64	0.54	1.31	121

In terms of total daily produced data the above Table 1 translates to :

- Focal Plane Frames : 525312 equivalent to 4.41 TBytes
- Raw Lines : 10.80 GByte

The above numbers are to be compared with an available downlink budget of 290 Gbit/Day showing that consistent on-board effort to reduce the volume of data products must be taken on flight.

3. SUPPORTING HARDWARE AND REAL-TIME PROCESSING

The supporting Hardware[1,7] for the Focal-Plane handling and data processing activities is in advanced phase of construction with some parts like the off the shelf CPU (Maxwell 750), the Dual Ported/Double Buffered transit memory (DPM) and one H2RG/SCE Digital Control Unit (DCU), already available for tests and application software (ASW)

*carlotta.bonoli@oapd.inaf.it; phone +39 049 8293481; fax +39 049 8759

development. The hardware is subdivided in two identical Data Processing Units (DPU) each one connected via MIL1553 bus to a supervisor Instrument Control Unit (ICU).
Next Figure *2* shows the basic HW structure for one DPU section from the two mounted on NISP. Each DPU section will drive half NISP focal-plane, namely 8x triplets: H2RG detector, SCE (Sensor Chip Electronics, the NISP version of the Teledyne Sidecar ASIC) and DCU.

Each single DPU is completely redundant against the 8x detection triplets so the only single point failure element is the single detection triplet itself. Exposures are programmed in broadcast mode on the two DPUs, following Figure 1 and executed in parallel and tight synchronization on each triplet, by dedicated synchronization hardware, in order to minimize possible random crosstalk effects.

Frame data from programmed MACC exposures are delivered in parallel to the DCU units where there is enough installed memory to numerically average group of readouts in single frames delivered to the Dual Ported/Double Buffered Memory collocated on the PCI addressing space covered by the local CPU. The DCU internal co-adding arithmetic works at 24 bits allowing up to 256 readouts per group be summed without overflow.

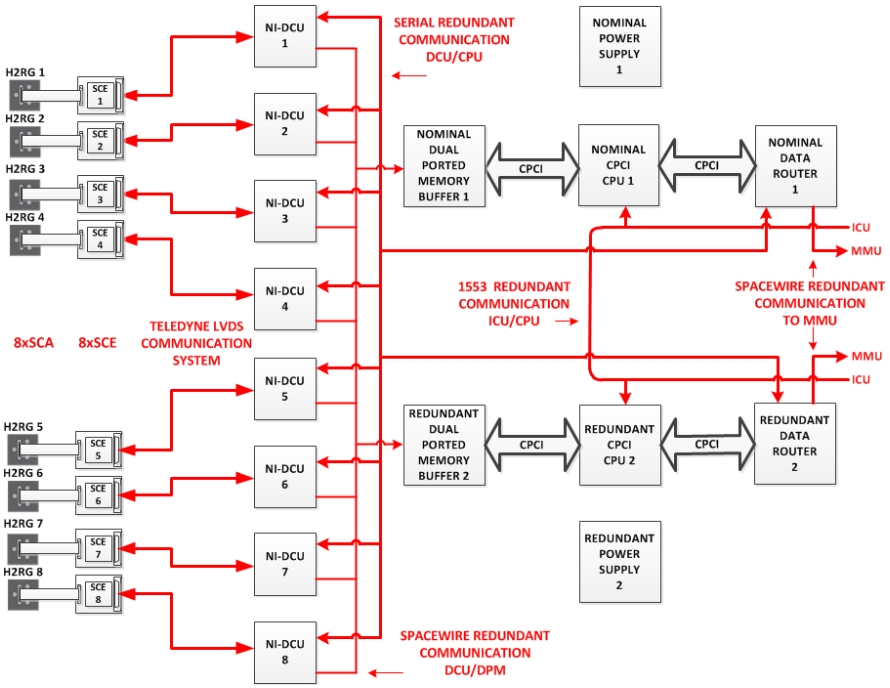

Figure 2. The NISP Warm-Electronics general Hardware, displayed 1x DPU section from two available handling a total of 8 + 8 detection triplets : H2RG Detector, SCE ASIC, DCU Control Electronics. Each DPU is redundant at level of CPCI hardware (Maxwell CPU, Data Router Board, Dual Ported/Double Buffer Memory and Main Power Supply).

This first averaging operation, covered in real-time by the DCU FPGA firmware, introduces a decimation of the native data amounts shown in Table 1 respectively to :

- Spectro Frames: 15x frames, 125.83Mbytes
- Photo Y: 4x frames, 33.56Mbytes
- Photo J: 4x frames, 33.56Mbytes
- Photo H: 3x frames, 25.17Mbytes

The above data amounts are stored by each DCU in the DPM in a single file per detector packed with the ‘raw-lines’ data and telemetry.

*carlotta.bonoli@oapd.inaf.it; phone +39 049 8293481; fax +39 049 8759

The DPM is also ‘dual-buffered’ and is constructed to allow the parallel storing from the 8x DCUs of up to 46 co-added groups in each buffer, this gives enough flexibility to program a dither sequence of exposures independently from the following processing. As an example the nominal survey sequence reported in Figure 1 foresees a maximum of 30x co-added groups to be stored on DPM during a specified sequence.
The presence of the double-buffer allows a complete decoupling of the DCU real-time operation from the subsequent CPU, deferred-time, processing operation along the dither sequence of exposures.

All the processing steps are directly performed by C code running on the CPU board core-memory supported by a triple-redundant Power-PC 750 set running at a clock speed of 4Mhz. In order to minimize the impact of the slow transfer speed, in particular for single R/W accesses, of the C-PCI bus hosting the Maxwell CPU and taking also into account the limited amount of memory available on the CPU (a total of 256Mbytes), it is advantageous to transfer one detector exposure data-set (co-added frames, raw-lines stack and telemetry) at a time for processing inside the CPU memory, this transfer is made in DMA (16Mbytes/S speed) iterating on the 8x detector exposures under CPU control.

The full ‘pipe-line’ of sequential steps performed to process the frame-data produced by focal plane programmed exposures are detailed in Figure 3, where the separation created at DPM between DCU ‘real-time’ and CPU sequential operations is well evidenced.

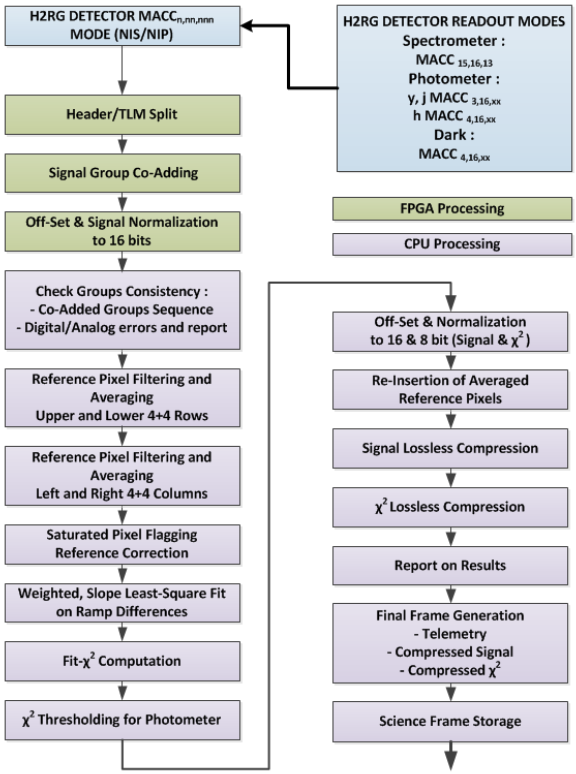

Figure 3. On-Board processing steps iterated on each detection channel (8 x triplets) upon reception of the programmed exposure frames on Dual Ported Memory. The first section in Figure is performed, in real-time, in FPGA HW while the CPU section is performed in deferred time.

In force of the DPM decoupling action the processing inside the faster CPU core memory and data-cache can be organized per single pixel exposure-ramps instead of frames, as in the DCU ‘on the fly’ operation, resulting in a better achievable algorithm efficiency.

*carlotta.bonoli@oapd.inaf.it; phone +39 049 8293481; fax +39 049 8759

4. DATA FRAMES CPU PROCESSING

The deferred time processing performed by the CPU on a given detector exposure starts from the correction of frame non-uniformities and pixel-correlated artifacts introduced by, as an example, different video-channels gain/offsets and detector line random offsets. This is obtained subtracting the reference vertical and horizontal detector pixels after median filtering and zonal averaging. The aim here is to correct sensitive pixels and to not propagate reference pixels artefact on the real pixels after subtraction, one typical case can be the presence of cosmic events on the same reference pixels.

At this level also saturated pixel ramps (2^{16} ADU counts) are flagged for no further processing and forced to the saturation value on the final output file.

The exposure final signal extraction follows three different threads on the base of the number of programmed groups:

- 1x single group: the frame is passed untouched to the compression. This is the case of some calibration exposures
- 2x groups: the frames are processed for usual Fowler mode and passed to the compression. This is the case of short time exposures
- More than 2 groups: the frames are processed with linear fit interpolation.

The core of the processing for most of the science exposures is a linear Weighted Least Square Fit on the signal discrete derivatives, with still present a Fowler option for the shortest exposure photometric modes.
Practically for all detector pixels signal ramps S_i where $i = 1 \dots M$ is the index of the M uniformly spaced groups the differences ramp $\Delta_i = S_i - S_{i-1}$ is taken and the slope b and χ^2 estimator are there computed. Obviously the sequence Δ_i is de-trended in respect to the original signal ramp and to the correlated part of photon noise. A computation of the fit intercept, representative of the detector pedestal level, is not possible and this important estimate is independently obtained from the original reference pixels and transmitted to ground.
Formulas for slope b and χ^2 estimator are taken for time uniformly spaced samples, where the time coordinate is simplified in the $i = 1 \dots M$ integer sequence. For the noise weighted case:

$$b^2 = \frac{\sum_i \left(\Delta_i + 2 \times \frac{\sigma_r^2}{N}\right)^2}{M - 1}$$

basically, on the discrete differences domain, the slope is reduced to a quadratic average, while the χ^2 is obtained in straightforward way by:

$$\chi^2 = 2 \times \left((M-1) \times b - (S_M - S_1) - 2 \times \frac{\sigma_r^2}{N} \times (M-1) \right)$$

Where:
M = number of MACC groups
N = number of samples per group
S_i = signal value at group-sample i
Δ_i = fitted signal differences
σ_r = read noise (RON) in ADU *rms*

The b slope formula for the derivative domain can be compared to the classical unweighted linear fit:

$$b = \frac{Cov(X,Y)}{Var(X)} = \frac{\sum_{i=1}^{M} (X_i - \overline{X})(Y_i - \overline{Y})}{\sum_{i=1}^{M} \left(X_i - \overline{X}\right)^2}$$

*carlotta.bonoli@oapd.inaf.it; phone +39 049 8293481; fax +39 049 8759

showing a consistent computational simplification in terms of per-sample operations. However, this is at the expense of a lower achievable *SNR* under identical MACC parametrization and at very low detector signal due to the differentiation operation, but this is not the NISP case where all the observations are photon noise limited.

Under nominal operation at the end of the pipeline two different frames are produced, one containing the computed signal for each pixel (ADUs, 16x bits) and one containing the computed χ^2 for each pixel. The χ^2 frame is decimated to 8x bits in the Spectrograph case and to 0/1 packed Booleans for the Photometer upon comparison with a programmable threshold.

The achieved data on-board decimation at this stage is:

- Spectro Frames: 1x result plus χ^2 frames, 12.57 Mbytes
- Photo Frames: 1x result plus χ^2 frames, 8.89 Mbytes

5. FINAL FRAME COMPRESSION

The last processing step before packaged file transmission to the Spacecraft Mass Memory (See Figure 3) is the data lossless compression. This is applied both to the final detector frames and to the Spectrograph/Photometer χ^2 frames. The algorithm used is an adapted version of the compression tool of the 'cfitsio' public library (http://heasarc.nasa.gov/fitsio/fitsio.html), based on standard Rice algorithm. Achieved compression ratios are here shown only for the final data frames being the achieved results on the already 'compressed' χ^2 frames (8 bit and 1 bit cut-off respectively for Spectrograph and Photometer) typically modest.

Compression tests have been done in two steps:

1. On simulated data, to have a first estimate of the reachable compression factors
2. On real data to confirm/modify the first estimates using the different exposure parameters and illumination levels foreseen during flight operations

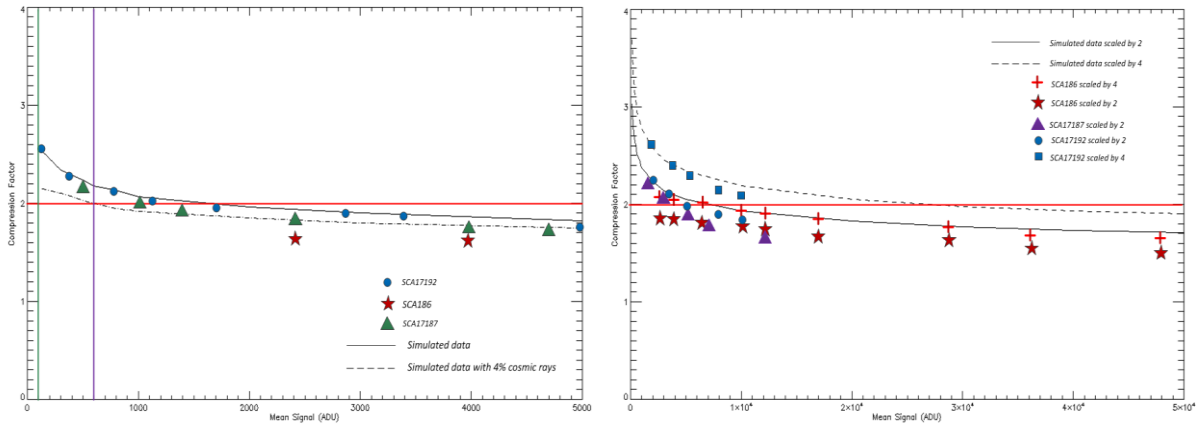

Figure 4. Plot of the compression factor versus the mean pixel signal for low and high signal level scales. Represented data are obtained from simulations, with and without cosmic rays added, and real H2RG data obtained during the NISP detectors pre-evaluation phase for three different detector samples. The red horizontal line is the reference NISP compression factor of 2 while the vertical bars in the left plot are representative for the Photometer and Spectrophotometer expected average background. On the right plot the effect of the application of a pre-scaling factor (2 and 4) on the data before compression.

*carlotta.bonoli@oapd.inaf.it; phone +39 049 8293481; fax +39 049 8759

Image data produced by multiplexed detectors present some challenges in achieving reasonable lossless compression factors. Considering the pedestal data produced by the non-illuminated detector one must consider the contribution of KTC noise residual, the usual RON and also the large/small scale variations induced by the different readout systems (Video lines, pixel-cell circuitry) or cosmic ray induced spikes. When the detector is illuminated different effects, apart the science image to be retrieved, are present. In particular, depending on the illumination level and on the detection system selected analog gain, the limiting factor to the achievable compression can become the photon noise and the detector cosmetics (blind/dead pixels, small-large scale QE variation). Often the lossless compression attempt of real IR detector frames can result in a frustrating experience.

Figure 4 shows the compression factor achieved for the different available data sets at increasing signal level. Simulated data[4] were generated without and with a 4% cosmic rays added as assumed usual for a spectrograph exposure on L2. Data were processed in the standard NISP way as previously described.
The left panel of Figure 4 shows also the expected background for the spectrograph case (violet vertical line, at about 600 ADU) and for the photometer case (green vertical line, at about 200 ADU).
On both panels the red horizontal bar is representative for the reference, average compression factor of 2.

Real data used on the presented tests are obtained with a conversion factor of 0.7 ADU/e^-, driven by an SCE video amplifier gain of 18 dB (8x).

The obtained plots in Figure 4 shows several aspects of the problem :

- The attainable compression factor is strongly dependent on the level of present ADUs noise, I.E. to the background illumination level for the NISP case. The classic square-root behavior of photon noise is well evident.
- Good quality detectors such as the SCA192 sample exhibits attainable compression factors behavior, at different illumination levels, quite compatible with those obtained from pure simulated data (only RON plus photon noise[4])
- The behavior of simulated data compression factor is quite compatible with the model described by the relation[6]:

$$CmpRatio = {BIT_{pix}}/{(N_{bits} + K)}$$

with BIT_{pix} the number of available bits for signal coding (16), and N_{bits} the fraction of bits per pixel covered by total noise σ_t (RON plus photon noise), given by:

$$Nbits = log_2\left(\sigma_t \sqrt{12}\right)$$

in the assumption of uniform statistics. N_{bits} is usually considered as a measure of the image 'entropy' and K a parameter giving a measure of the efficiency of the compression algorithm. Typically, Rice based algorithms behave as with K=1.

The first conclusions are:

- Considering the science exposures it appears possible to reach the specified average compression factor of 2 up to a level of 1K ADUs, depending also on the number of collected cosmic glitches, without digital pre-scaling
- Considering the calibration exposures, especially flats and linearity test exposures spanning the full dynamics of the system, it is necessary to introduce a digital pre-scaling factor in order to reduce the impact of the photon noise and to stay within the specified average compression limits

The final achieved image-data on-board decimation at the end of the pipe-line processing and before transmission to the spacecraft Mass Memory is on the base of the average attainable compression factors:

*carlotta.bonoli@oapd.inaf.it; phone +39 049 8293481; fax +39 049 8759

- Spectro Frames: 1x result plus χ^2 frames, 6.29 Mbytes
- Photo Frames: 1x result plus χ^2 frames, 4.44 Mbytes

This means that, on the average, considering also the extra ancillary data (basically telemetry and 'raw monitoring lines'), 24 hours of nominal survey will produce a total of 291.38 Gbits considering the complete 16x detectors focal plane.

6. RESULTING PROCESSING TIME

Table 2 reports the processing times evaluated for 8 detectors as measured on a Maxwell 750 board running at 4 Mhz clock. The table organization is: on the leftmost column each processing step, on the top row, each instrument exposure mode. Estimated times are for the nominal science mode.

Table 2. Processing time (Seconds) measured on Maxwell 750 for 8x processed H2RGs detectors as in the 4th dither (1323s total Dither time, See Figure 1).

Processing Step	Spectro 15 Groups	Photo Y 4 Groups	Photo J 4 Groups	Photo H 3 Groups	Dark 4 Groups	Total
Linear Fit on Group-Frames Ramp + Ref Pixels Correction	100	51	51	47	51	300
Lossless Compression for slope and χ^2 frames	9	6	6	6	6	33
Total (Seconds)	109	57	57	53	57	333

In order to cope with the limited amount of memory available on the Maxwell CPU (256 Mbytes) the processing is currently iterated 8x times on a single detector data-sets making use of real detector frames, preloaded on the CPU memory through the operating system (VxWorks) file-system. In the same way the final processed results are extracted and compared, after de-compression, for correctness check, on an external computer where the same test data-set has been independently processed, exactly following the same pipe-line reported in Figure 3, but performed making use of standard data-processing tools (IDL data processing language).

The total amount of CPU core memory currently used during the nominal processing of 8x detectors is shown in Figure 5. It is expected to use part of the available margins during the next implementation of the DPU physical interfaces handling and for processing pipe-line improvements.

*carlotta.bonoli@oapd.inaf.it; phone +39 049 8293481; fax +39 049 8759

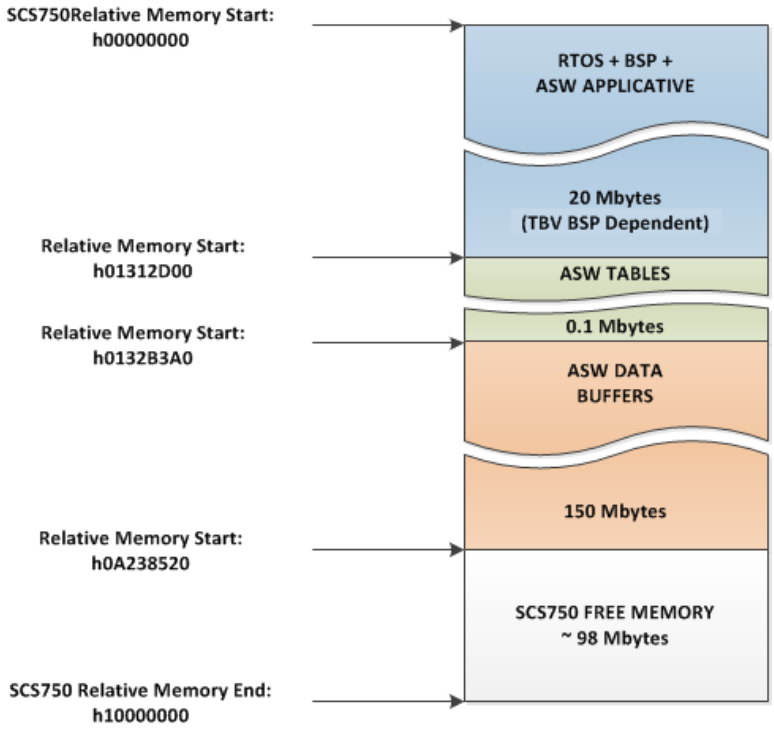

Figure 5. Present DPU peak memory use during NISP nominal operations with the full processing pipe-line implemented.

7. CONCLUSIONS

The overall concept for the handling of the NISP IR focal-plane detection system at HW and SW level has been presented. Part of this system is based on space qualified FPGA HW taking care of control and real-time operations on incoming data while most of the on-board processing pipe-line is implemented on sequential, space qualified, processor boards.

On a prototype hardware, compatible with final NISP in flight system, a complete processing pipe-line based on a simple linear fit algorithm and a lossless data compression algorithm have been adapted and tested using simulated and real detector data coming from the NISP detector pre-evaluation phase.

The fit algorithm has been generalized to cover the needs for the focal plane spectrometer and photometer modes, requiring significant differences on the exposure parametrization and on the specific processing.

The lossless data compression algorithm has been derived from widely used astronomical standards introducing more flexibility in the handling of the wide dynamical range covered by the science and calibration images produced.

Tests and end-to-end verifications have been made using common, real detector data sets, and directly comparing products produced by different systems, the NISP model and standard data processing tools, implementing the same processing pipe-lie.

ACKNOWLEDGMENTS

We acknowledge the financial support from contract ASI/INAF 1/023/12/1. Thanks are due to CGS (IT) and Maxwell (US) companies for kind helpfulness preliminary performance tests and HW development.

*carlotta.bonoli@oapd.inaf.it; phone +39 049 8293481; fax +39 049 8759

REFERENCES

[1] Maciaszek, T. et al., “Euclid Near Infrared Spectro Photometer (NISP) instrument concept and first test results obtained for different breadbords models at the end of phase C”, this conference

[2] Rauscher, B. et al., “Detectors for the JWST Near-IR Spectrograph. I. Readout Mode, Noise Model and Calibration Considerations,” PASP 119, 768-786 (2007)

[3] Beletic, J.W., Blank, R., Gulbransen, D., Lee, D., Loose, M., Piquette, E. C., Sprafke, T., Tennant, W. E., Zandian, M. and J. Zino, “Teledyne Imaging Sensors: Infrared imaging technologies for astronomy and civil space”, Proc. SPIE 7021(20), (2008)

[4] Bonoli, C., Bortoletto, F., Giro, E., Corcione, L., Ligori, S. and Nicastro, L., "A Frame Simulator for Data Produced by ‘Multi-Accumulation’ Readout Detectors", Proc. SPIE 7731, 77312U (2010)

[5] Laureijs, R.J., et al., "Euclid: ESAs mission to map the geometry of the dark universe", Proc. SPIE 8442, (2012)

[6] Pence, W.D. et al, “Lossless Astronomical Image Compression and the Effects of Noise “,PASP, 121, 414, (2009)

[7] Prieto, E. et al., “Euclid near-infrared spectrophotometer instrument concept at the end of the phase A study”, Proc. SPIE 8442, (2012)

*carlotta.bonoli@oapd.inaf.it; phone +39 049 8293481; fax +39 049 8759